

**Quasi Periodic Oscillations (QPOs) and frequencies in an accretion disk  
and comparison with the numerical results from non-rotating black  
hole computed by the GRH code**

Orhan Donmez

*Nigde University Faculty of Art and Science, Physics Department,  
Nigde, Turkey 51200\**

Received (Day Month Year)

Revised (Day Month Year)

The shocked wave created on the accretion disk after different physical phenomena (accretion flows with pressure gradients, star-disk interaction etc.) may be responsible observed Quasi Periodic Oscillations (QPOs) in  $X$ -ray binaries. We present the set of characteristics frequencies associated with accretion disk around the rotating and non-rotating black holes for one particle case. These persistent frequencies are results of the rotating pattern in an accretion disk. We compare the frequency's from two different numerical results for fluid flow around the non-rotating black hole with one particle case. The numerical results are taken from our papers Refs.1 and 2 using fully general relativistic hydrodynamical code with non-selfgravitating disk. While the first numerical result has a relativistic tori around the black hole, the second one includes one-armed spiral shock wave produced from star-disk interaction. Some physical modes presented in the QPOs can be excited in numerical simulation of relativistic tori and spiral waves on the accretion disk. The results of these different dynamical structures on the accretion disk responsible for QPOs are discussed in detail.

*Keywords:* Black hole, accretion disk,  $X$ -rays, QPOs, frequencies

PACS Nos.: include PACS Nos.

## 1. INTRODUCTION

Observed properties of the high frequency from  $\approx 1$  Hz to  $\approx 1$  kHz quasi periodic oscillations in the X-ray light curve of the black hole and the neutron star binaries have been studied by <sup>3</sup> and <sup>4</sup> and references therein. The studies of high frequency variability in  $X$ -ray binaries provide a unique opportunity to explore the fundamental physics of space time and matter. The dynamical timescale on the order of several milliseconds is a timescale of the motion of matter through the region located in close to black hole. Thus, Theories of the physics of the inner accretion disk, the orbital motion of matter in relativistic gravity and the relativistic disk oscillations can be probed by high frequency signals from black hole binaries. The

\*electronic address:odonmez@nigde.edu.tr

2 *Donmez, O.*

observation of high frequency properties have been motivated the theory of relativistic “diskoseismology” which studies the hydrodynamical oscillation modes of geometrically thin accretion disk for one particle case<sup>5, 6</sup>. Different types of shock waves, standing two-armed spiral shock, moving one-armed shock and tori<sup>(1, 2, 7, 8, 9)</sup>, with discrete and different range of frequencies can exist in such disk because the radial profile of general relativistic matters oscillation frequencies can create finite region where modes are trapped.

QPOs produced on the accretion disk in the black hole systems are thought to arise from physical processes. Depending on the where the oscillation reside, the various accretion models can be seen. These models are relevant to our understanding of various physical radii in the binary systems that are associated with high frequency variability according to the some theories. Some of these models accommodate movements of the inner accretion disk that are proposed to explained the change in the frequency of high frequency QPOs.

However, radial pressure gradients themselves can permit the existence of discrete modes because they produce a disk, or torus, of finite extent. At least in the case of black hole  $X$ –ray binaries, QPOs are only observed in the power law spectrum states in which the flow is not solely composed of a geometrically thin accretion disk. Therefore, it is believed that the radial pressure gradients may be responsible for trapping different frequencies modes on the accretion disk. Those reported have recently explored low frequency<sup>10</sup> and high frequency<sup>11, 12</sup> that accretion disk may explain observed QPOs. Geometrically thick tori may form in stellar collapse, and modes of dense tori around black holes have also been suggested as a detectable source of gravitational waves<sup>13</sup>

The first part of the paper provides the theoretical background on the physics of  $X$ –ray binary system frequency variability which is presented in accretion disks around the black hole for one particle system. This frequencies arise rotating patterns in the accretion disk and shock waves created on it and driven by gravity of black hole. Second part of paper compares the numerical simulation results computed from fully general relativistic hydrodynamics code with one particle case. We also report the different modes on numerical modeled accretion disk around the non-rotating black hole.

## 2. Characteristic Disk Frequencies

The characteristic frequencies of this ring depend upon whether the spin axis of the ring is tilted with respect to the spin axis of the black hole. If we have a ring of matter orbiting a black hole that is itself spinning. Characteristic frequencies also depend upon the mass of the black hole,  $M$ , angular momentum of the black hole,  $J$ , and the radius of ring,  $r$ . The artistic representation of the frequencies is shown in Fig.1. The motion of a test particle in nearly circular orbits close to equatorial plane around a Kerr black hole can be decomposed into three components, which are circular planar motion at the orbital frequency  $\nu_\phi$ , harmonic radial motion at

the radial epicyclic frequency  $\nu_r$ , and harmonic vertical motion at the meridional epicyclic frequency  $\nu_\perp$ <sup>15</sup>.

A test particle has an orbital frequency  $\nu_\phi$ , measured by static observed at infinity<sup>14</sup> called the Keplerian rotational frequency. This is the frequency at which matter rotates about the black hole, if the ring and black hole spin axis are aligned and given by

$$\nu_\phi = \frac{1}{2\pi} \left( \frac{M^{1/2}}{r^{3/2} + aM^{3/2}} \right). \quad (1)$$

where the geometrized units  $c = G = 1$  are used,  $r$  is the orbital radius and  $a$  is the dimensionless black hole spin parameter ( $a = cJ/GM^2$ ). We compute the theoretical and numerical calculation in dimensionless units scaled by black hole mass  $M$  in the rest of the paper. The distances and times are measured in units of  $GM/c^2$  and  $GM/c^3$ , respectively.

The radial epicyclic frequency  $\nu_r$  is the frequency at which a particle oscillates about its orbit if it is given radial 'kick'. The radial epicyclic frequency is zero at the inner edge of the disk, rises to a maximum near the disk inner edge, and then falls off and is equal to Keplerian frequency at large radii. This falls off in frequency at the inner edge of the disk is a consequence of general relativity and strong field gravity. It can be defined on the observer far from disk and given by

$$\nu_r^2 = \nu_\phi^2 \left( 1 - \frac{6M}{r} + \frac{8aM^{3/2}}{r^{3/2}} - \frac{3a^2M^2}{r^2} \right). \quad (2)$$

The vertical epicyclic frequency  $\nu_\perp$  corresponds to the vertical perturbation of particle, rotating in a circular orbit around the black hole

$$\nu_\perp^2 = \nu_\phi^2 \left( 1 - \frac{4aM^{3/2}}{r^{3/2}} + 3\frac{a^2M^2}{r^2} \right). \quad (3)$$

In Fig.1,  $\nu_{LT}$  : the Lense-Thirring frequency is the frequency at which the spin axis of the ring and the spin axis of the black hole precess about the total angular momentum, dominated by the black hole, if these axes are not aligned. The Lense Thirring frequency is only comparable to the Keplerian orbital frequency for rapidly spinning black holes.

In the Newtonian theory of spherically symmetric gravitating bodies (in the absence of Keplerian mechanics), the three frequencies coincide ( $\nu_\phi = \nu_r = \nu_\perp$ ) but in the relativistic theory  $\nu_\phi > \nu_r$ . The degeneracy of epicyclic frequencies are broken by general relativistic effects. The all three frequencies are defined for rotating black hole. In case of non-rotating black hole, Schwarzschild, the frequencies are  $\nu_\phi = \nu_\perp > \nu_r$ . The radial dependences of these frequency for a test particle in a rotating and non-rotating black hole is illustrated in Fig.2. The vertical frequency equals to orbital one in case of non-rotating black hole. The rotating

matter can be deviate around the minimum precession frequency, seen in Fig.2. Accounting a QPO frequency with a Keplerian frequency provides restriction on the relationship of the black hole mass and the angular momentum for a given radius. The radius can be radius of marginally stable orbit, or any other physical radius of a region associated with the excitation of the QPO. The circular orbits close to black hole are unstable and last stable circular orbit (LSSO) is located where  $\nu_r^2$  vanishes. As with the Schwarzschild black holes, the last stable orbits for a Kerr black hole are the circular orbits closest to the event horizon. Objects in orbit inside of the last stable orbit fall onto the event horizon. The Fig.3 shows the LSSO as a function of spin parameter  $a$  for clockwise orbit. LSSO tends to 1 while the black hole spin goes to rapidly rotating black hole spin, 1.

One of the fundamental trapping oscillation has been identified by internal gravity, called the  $g$  mode. The  $g$ -mode oscillations involve predominantly vertical displacements of the disk and are mainly regulated by centrifugal and pressure gradient forces. The are trapped near the maximum of the radial epicyclic frequency in the resonant cavity, seen in Fig.2. The  $g$  mode should become trapped in the potential well of accretion disk (geometrically thin) in a black hole potential. The depth and size of region depend where the modes are trapped depends on both the mass and the spin of the black hole.

Black hole can make a close orbit in case of orbital and epicyclic frequencies are same. Because of general relativistic effects, the frequencies are in general different and the orbits will precess. The orbits of particles that are eccentric and slightly tilted with respect to the radial are involved. On the other hand, particles in slightly tilted orbits fail to return to the initial displacement from the equatorial plane in radial direction, after a full revolution around the black hole. This introduces a

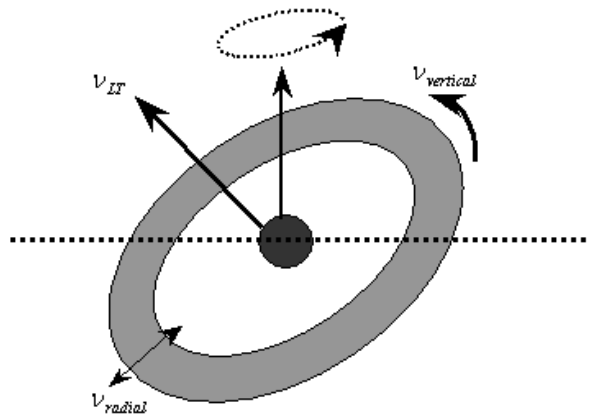


Fig. 1. Artistic visualization and representation of accretion disk black hole binary system and their frequencies.

precession frequency and define with  $\nu_{prec} = \nu_{orb} - \zeta \nu_{rad}$  where  $\zeta$  defines orbit,  $n/m$ <sup>16</sup>. The integers  $n$  and  $m$  determine the shape of the precession orbit. Fig.4

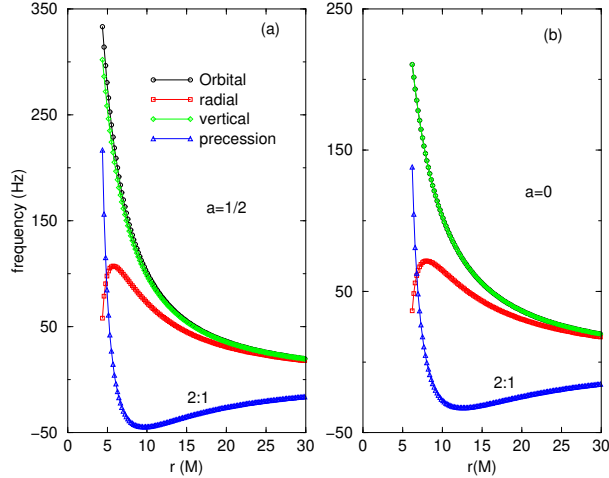


Fig. 2. Orbital frequency  $\nu_\phi$ , radial epicyclic frequency  $\nu_r$ , vertical oscillations frequency  $\nu_\perp$  and precession frequency  $\nu_p = \nu_\phi - 2\nu_r$  of a 2:1 orbit in an accretion disk around (a) a Kerr black hole with  $a = 1/2$  and (b) a Schwarzschild black hole for  $M = 10M_\odot$ . (a) Precession frequency exhibits a shallow negative minimum at  $r_* \approx 9.65(142.1km)$  and the last stable circular orbit is located at  $r = 4.21(62.089km)$ . (b) Precession frequency exhibits a shallow negative minimum at  $r_* \approx 12.42(183.25km)$  and the last stable circular orbit is located at  $r = 6.0(88.48km)$ .

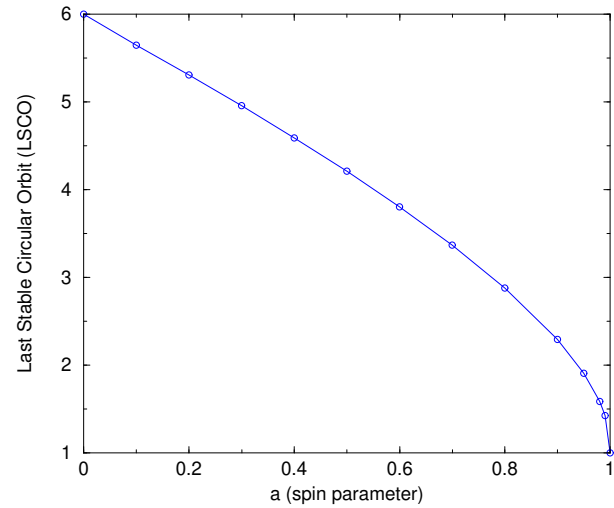


Fig. 3. The last stable circular orbit (LSCO) in the accretion disk around the Kerr black hole vs. its spin parameter is plotted.

6 *Donmez, O.*

plots the precession frequency as a function of radial coordinate for different mode. We have computed minimum values of precession frequency location. The negative minimum value of precession gets bigger and their location goes to black hole LSCO in case of bigger rotation number at fixed epicycle in an accretion disk around the Kerr black hole with the spin parameter  $a = 0.5$ . In the relativistic precession models, QPO frequency variations for a black hole are considered to be due to variations in the locations of the inner edge of the accretion disk.

Until now, we present the test particle epicyclic frequencies and their properties depend on black hole spin. We only focused on the kinematics and neglected particle interactions and the hydrodynamical effects of the disk. In a real accretion disk, the collective particle motion would have to be excited by some dynamical mechanism. It complicates and requires numerical simulations of the disk to fully understand the driving process, and the effects of the hydrodynamical forces and pressure jumps. In the next section, we present and discuss the oscillating properties of relativistic, non-selfgravitating tori and one-armed spiral shock wave created in the accretion disk around the black hole <sup>1,2</sup>.

### 3. Numerical Results

The characteristic frequencies defined for one-particle system are also important in a discussion of fluid motion about a gravitating body in the general relativity<sup>17</sup>. The accretion disk is a body of hot gas in some regions that supported against infall primarily by rotation and is nearly hydrostatics equilibrium. The theories of accretion admit solutions in which the disk thickness is much smaller than its radial

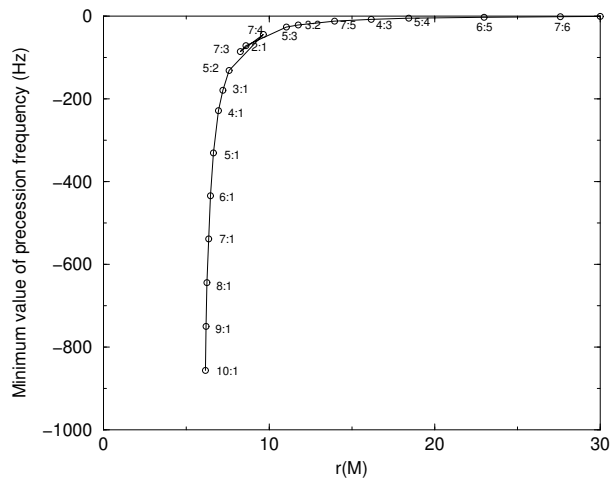


Fig. 4. Precession frequency exhibits a shallow negative minimum value for different orbits in an accretion disk around a Kerr black hole with  $M = 10M_\odot$  and  $a = 0.5$ . While the rotation number increases in case of a fixed epicycle, the location of precession frequency decreases.

extent, but also solutions in which the disk has the geometry of a torus. Like other extended bodies in equilibrium, the disk capable of motion in a variety of modes. The radial vibrations of two-dimensional models of geometrically thick disk have been investigated numerically in the Schwarzschild black hole<sup>18</sup>.

It is pointed out that in general relativity, in addition to the fixed frequencies, orbital, radial and vertical, there are other preferred frequencies, those of 2:1, 3:1, etc., resonances between orbital and radial epicyclic frequencies. These are possible because the ratio of orbital and radial epicyclic frequencies tends to large values near the marginally stable orbit:  $\nu_\phi/\nu_r \rightarrow \infty$  as  $r \rightarrow 6M$  for non-rotating black hole, seen in Fig.2. Frequencies in 2:1 or 3:1 ratio can be in resonance because epicyclic motion is enharmonic. As a usual for non-linear oscillators, the resonance occurs for a range of frequencies near the eigenfrequency of the oscillator, so the orbital frequency need not be an exact multiple of the eigenfrequency of the epicyclic oscillator, nor need it be constant. Here, we show the different frequencies and their ratios produced from two different numerical results, toris created around the black hole and one-armed spiral shock wave formed as a consequence of star-disk interaction.

### 3.1. *Torus created close to black hole*

To briefly summarize the basic properties of the oscillating torus model, we recall that we are considering a non-selfgravitating perfect fluid toris orbiting around the non-rotating black hole<sup>1</sup>. The fluid is rotating in a circular non-geodesic motion and the equations of relativistic hydrodynamics in a Schwarzschild black hole space-time are solved using the general relativistic hydrodynamics code described in Ref.19. The introduction of the harmonic oscillations of the torus having centrifugal and pressure-gradients as the restoring forces. The restoring forces can explain toris dynamic of accretion disk. A first restoring force is the gravitational force in the direction vertical to orbital plane and which will make a harmonic oscillation on equatorial plane. Second force is provided by the pressure gradients. Third restoring force known as centrifugal force is responsible for internal oscillations of the orbital motion of the disk and the marginally bound motion produces epicyclic frequencies.

In a real accretion disk, the collective particle motion would have to be excited by some dynamical mechanism. It complicates and requires numerical simulations of the disk to fully understand the driving process. In Fig.5, we give the results of vertical epicyclic frequency from numerical simulation of accretion disk around the Schwarzschild black hole using General Relativistic Hydrodynamic (GRH) code<sup>1, 9</sup> and a test particle. In the test particle case, we content with studying the kinematics only. We set off a collective mode by selecting appropriate initial conditions and follow the pattern evolution by tracing the motion of one particle. Self interaction of particle and hydrodynamical effects are neglected. In the numerical simulation case, we have all effects except the self gravity. Contrast to Ref.23 for neutron star, it is seen in the Fig.5 that orbital epicyclic frequency in a perfect fluid disk case

is sup- or super-Keplerian depends on the radial location for the same black hole mass, seen in Fig.6. So the deviation of the these frequencies using same black hole may come from the omission of hydrodynamic effect for a test particle. Fig.5 shows the orbital frequency of toris rotating around the Schwarzschild black hole of mass  $M = 10M_\odot$  as a function of radial coordinate. We find that the torus performs harmonic oscillations both in the radial and vertical directions. Both these oscillations speak of a non-linearity in the system. Orbital frequency for a test particle and numerical result for fluid are plotted on the same graphics and they are comparable. The fluid in the accretion disk has rotated oscillation frequency depends on the radial dependence. While the matter inside the  $r = 28M$  rotates with super-Keplerian frequency, it is sup-Keplerian in the outside this radius, seen in Fig.6. The disk which rotates super-Keplerian frequency has strong centrifugal force and it is balanced by strong gravity close to black hole. As a consequence of this phenomenon, the tori is created around the black hole. The gas pressure dominates radiation pressure throughout the disk except (depending upon parameters) in the innermost regions where the temperatures are high and it is outside the  $r = 28M$ . Fig.7 shows the radial frequency from numerical result of tori and a test particle case. They have a similar behavior but numerical results have more oscillatory motions because of some forces which would not produced in the test particle case and numerical errors. The numerical errors are produced using with low resolution in numerical simulations. Using the high resolution is not possible in this case because we have to wait until  $t \approx 37000M$  to reach steady state. The strong gravity is responsible for the presence of two frequencies  $\nu_\phi \neq \nu_r$ , seen in Figs.5 and 7, where in Newtonian gravity there is only one frequency ( $\nu_r = \nu_\phi = \nu_\perp$ ).

The transition from a Keplerian to a sub-Keplerian flow may proceed smoothly, although it is very likely that a perfect adjustment never occurs. In general, the transition should take place through the setting up of a centrifugal barrier (where a centrifugal force slightly exceeds the gravitational force) within the adjustment radius. Inside potential barrier, matter can be held and produces a tori close to black hole. Here we discuss the formation of kinks and shocks in the supersonic regime of accretion flow (in tori) as a possible physical reason for a super-Keplerian rotation. In a region, seen in Fig.6, with super-Keplerian rotation matter may experience the relaxation oscillations in radial directions. These oscillations are expected to be in a resonance with the local angular velocity in a disk, and the variation in an emitting area caused by the oscillations around a transition point produces the quasi-periodic oscillations (QPOs) in the X-ray flux. The relatively soft disk photons in a centrifugal barrier region are scattered off the hot electrons thus forming the Comptonized X-ray spectrum. The electron temperature is regulated by the supply of soft photons from a disk, which depends on the ratio of the energy release (accretion rate) in a disk and the energy release in centrifugal barrier region. For example, the electron temperature is higher for lower accretion rates while for a high accretion rate (of order of the Eddington one) a centrifugal barrier region cools down very efficiently due to Comptonization.

The axisymmetric oscillation modes of relativistic tori consists of different modes. Parametric resonance between two oscillations is possible in accretion disk because the coupling of modes is non-linear in hydrodynamics. The ratio of orbital velocity to radial frequency is given in Fig.8. The radial mode oscillation as the origin of high frequency QPOs in black hole systems has been observed in the different frequency ratios  $1 : 2 : 3 \dots$  at different radial locations at a fixed  $t = 43712.61M$ . The frequency ratios  $5 : 3$  and  $3 : 2$  have also been noted in Refs.20 and 21.

The investigations of the oscillatory properties of non-selfgravitating tori orbiting around the black hole and their frequency ratios for different modes at different times are shown in Fig.9 after tori reached to steady state. The location of different ratios stay in one place with small oscillation around the  $10.2M$ . It produces consistent high frequency and it can be observed different  $X - ray$  detectors. Another important thing it can be seen here that twin high frequency ratios produced at each time step but they produce oscillatory behavior, seen in Fig.9. For the three microquasars GRO J1655-40, XTE J1550-564 and GRS 1915+105 twin high frequency quasi-periodic oscillations (HFQPOs) with a ratio of  $3 : 2$  and  $3 : 1$  have been measured<sup>22</sup>.

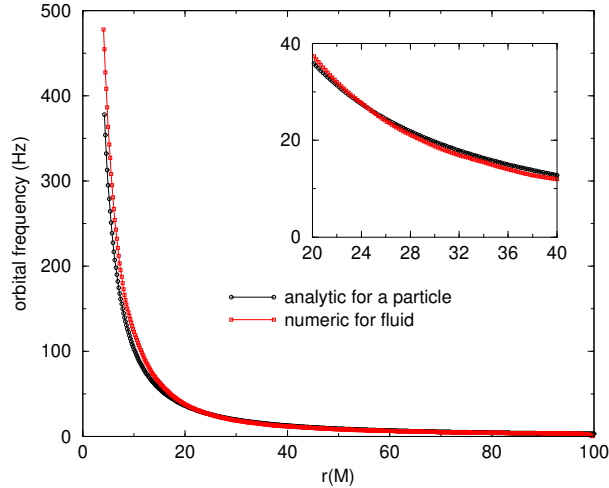


Fig. 5. Orbital frequencies plotted for analytic and numerical considerations as a function of radial dependence. Comparison of the orbital epicyclic frequency of a test particle with a perfect fluid disk case which is produced from fully general relativistic hydrodynamic code. The numerical results used here are taken from Donmez, 2006 (Submitted), seen in Fig.3 at  $t = 43712.61M$  which shows the created accretion disk and tori around the non-rotating black hole with mass  $M = 10M_{\odot}$ .

### 3.2. One-armed spiral shock wave created in case of star-disk interaction

The perturbed accretion disk around the non-rotating black hole created rotating one-armed spiral shock wave. This spiral shock wave transports the angular momentum out of disk when the matter collides with it and it causes the gas falling into the black hole<sup>7</sup>. Dynamically stable shock wave generally oscillates in a mixture of internal and global modes. Internal modes cause oscillations of the pressure and density profile at the shock front. The reflected flux is therefore directly modulated by the changes in the thermodynamical properties of the gas, while the dynamic of rotating shock wave is nearly unchanged.

The radial dependences of orbital (vertical) frequencies at different times and fixed angular distance,  $\phi = 0$  for a non-rotating black hole and accretion disk with rotating shock are illustrated in Fig.10. in the early time of simulations, orbital frequency of disk shows oscillatory behavior around the test particle orbital frequency and it diverges from the test particle case during the process when the gas is falling into black hole. The gas on the disk rotates smaller oscillatory velocity and it produces smaller epicyclic frequency.

Fig.11 shows the ration of orbital to radial frequency for one-armed spiral shock case at different radial fixed location at a snapshot,  $t = 9534.70M1M$ . While the frequency ratio at  $r = 4M$  and  $r = 6M$  do not exhibit any commensurate fre-

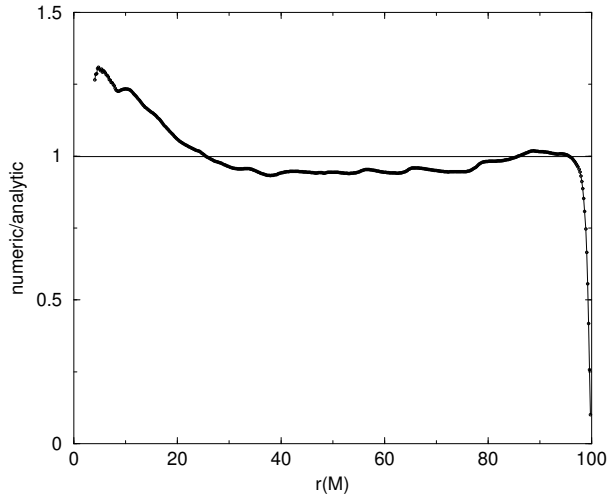


Fig. 6. Frequencies ratio of numerical result with analytic value as a function of  $r$  in Fig.5. If the ratio is bigger than 1, it represents the super-Keplerian disk which is rotating faster than Keplerian disk. Otherwise disk is sub-Keplerian.  $r = 25.37M$  represents the location where Keplerian velocity equal to orbital velocity of the fluid. Inside that radius, the disk has super-Keplerian angular velocity. The sub-Keplerian disk becomes puff-tuffed and geometrically thick in place where the disk is super-Keplerian.

quencies, the frequency ratio at  $r = 10.8M$  produces commensurate frequencies in different ratios, 3 : 1, 3 : 2, 2 : 1 etc. In the particular radius, different ratios can be found in orbital and radial coordinate frequencies. Commensurate QPO frequencies can be seen as a signature of an oscillation driven by some type of resonance conditions. Fig.12 shows the location of different ratios at a fixed radial coordinate  $r = 10.8M$  at different times. The oscillatory behavior of accretion disk produces consistent frequency ratio due to shock wave created. The location of 3:2 ratios stay in one place but it is moving in angular direction after one-armed shock wave created which moves around the black hole.

Difference between theoretical results for a fixed spin parameter with numerical results for a non-rotating black hole at different time steps are computed in Fig.13. The black hole and particles are corotating orbits, where the black hole spin parameter is positive. On the other hand, the black hole and particle are the counterrotating orbits, while the black hole spin parameter is negative. The numerical results are taken from in our paper Ref.7 for the non-rotating black hole. Fig.13(b) and (c) show that results of spinning black hole vertical frequency tends to numerical values. Because of tendency of numerical value to theoretical value for rotating black hole, even though we have started with accretion disk problem around the

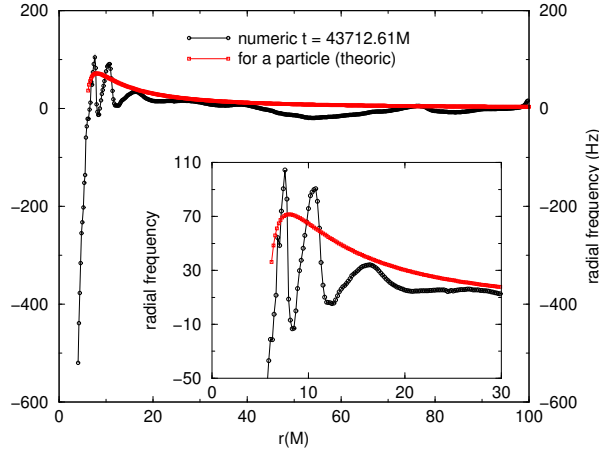


Fig. 7. Radial frequencies of the theoretical and the numerical results (same as Figs.5 and 6) as a function of radial coordinate. The numerical and theoretical results can be compared. The numerical radial frequency is oscillating close to black hole. The last stable circular orbit for both cases almost in same place. The fluid falls into black hole and goes faster and faster and nothing can escape to the outside world, not even light when the matter closes to black hole (horizon,  $2M$ ) in numerical simulation. On the other hand, particle radial frequency goes zero when particle reaches to last stable circular orbit for non-rotating black hole,  $6M$ . The radial epicyclic frequency reaches its maximum at  $r = 8M$  in theoretical consideration and  $r = 7.6M$  in numerical calculation for a non-rotating black hole and both go to zero at last stable circular orbit. This figure shows a luminous torus oscillating along its own axis.

non-rotating black hole, the black hole may have spinning because of the hydrodynamical effects. But the gap between theoretical and numerical results for the vertical epicyclic frequency in the the black hole which rotates in the counterrotating orbits gets bigger. This graphic gives big clue to explain that the non-spinning black hole may rotate due to effects which are created interactions. The transfer of mass and angular momentum from the disk to the black hole and interactions among them may lead to the gradual increase of the rotation law of the initially non-rotating black hole, Schwarzschild.

#### 4. Comparison with Observations

Until now, we have given numerical and theoretical results of epicyclic frequency in black hole binary system. The numerical results have produced two-different models, tori created around the black hole and one-armed shock wave created on the accretion disk as a result of star disk interaction. After this point, we compare the results from numerical calculations with observed one. We make comparison for the presence in the black hole X-ray source of observed stable frequencies, demonstrated as narrow-with QPOs. These oscillation is produced as a result of parametric reso-

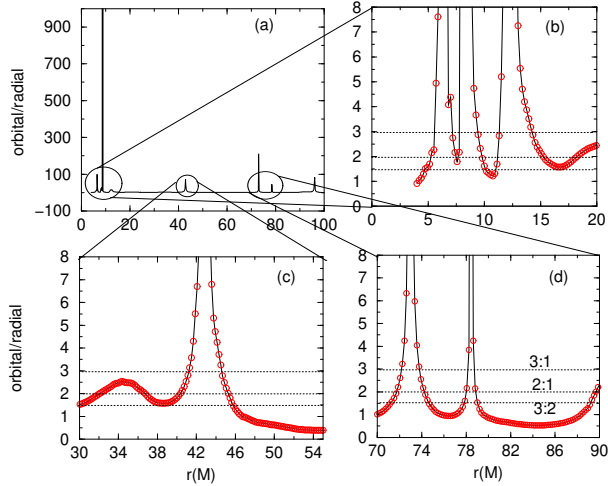


Fig. 8. The ratio of orbital to radial frequency to find out particular radius that corresponds to  $2:1$ ,  $3:1$  and  $3:2$  orbits, which are representative of the deformed and the self-intersecting orbit classes, in numerical calculation for a perfect fluid. The perfect fluid disk case produced from fully general relativistic hydrodynamic code. The numerical results used here are taken from Donmez, 2006 (Submitted), seen in Fig.3 at  $t = 43712.61M$  which shows the created accretion disk and tori around the non-rotating black hole. The mass of the black hole is  $M = 10M_{\odot}$ . (a) Represents the ratio of orbital to radial frequency as a function of radial coordinate. (b) Represents the same ratio but focused around  $0 < r < 20$ .  $3:2$  orbits found at  $r \approx 4.6M$ ,  $r \approx 10.11M$ ,  $r \approx 11M$  and  $r \approx 16.67M$ .  $2:1$  orbits found at  $r \approx 5.1M$ ,  $r \approx 7.5M$ ,  $r \approx 9.7M$ ,  $r \approx 11M$ ,  $r \approx 15.2M$ , and  $r \approx 18.18M$ .  $3:1$  orbits found at  $r \approx 5.45M$ ,  $r \approx 6.9M$ ,  $r \approx 7.74M$ ,  $r \approx 9.3M$ ,  $r \approx 11.22M$ , and  $r \approx 14M$ . The orbits radial locations in the (c) and (d) can also be seen.

nance in the accretion disk, and the observed frequencies ratios correspond to that resonance.

In this section we discuss the comparison of high frequency QPOs detected by RXTE in black hole binary candidate with numerical founded frequencies. High frequency QPOs at 40 – 450 Hz have been observed with RXTE for four black hole candidates. Furthermore, three of these sources show harmonic (3:2) pairs of frequencies. The models for these QPOs, orbital resonance and diskoseismic oscillations, invoke strong gravitational effects. In the inner accretion disk and they depend on the black hole mass. The vertical and radial frequencies ratios are given for numerical calculations in Figs.9 and 12. These figures represent different ratios, 3 : 2, 2 : 1, 3 : 1.... Some of the ratios are agreement with observed one. There are, possibly, two distinct groups among black hole binary candidate with the high frequency QPOs (in the  $\sim 100$  – 300 Hz range). In GRS 1915 + 105 and GRO  $J1655 - 40$  the QPO frequency is stable. The frequencies of the GRO  $J1655 - 40$  is the 450 Hz for vertical and 300 Hz for radial is has been argued by Ref.24 that high frequencies are sufficiently high that they require substantial black hole spin. For example, in the case of GRO 1655 – 40 the 450 Hz frequency exceeds the maximum orbital frequency at the innermost stable circular orbit around the non-rotating black hole, seen in Fig.5. The frequencies of the GRS 1915 + 105 has recently been found in the relevant 3 : 2 pair at 168 for vertical and 113 Hz for radial<sup>25</sup>. Figures 9 and 12 computed from numerical calculations show the stable high frequency QPO

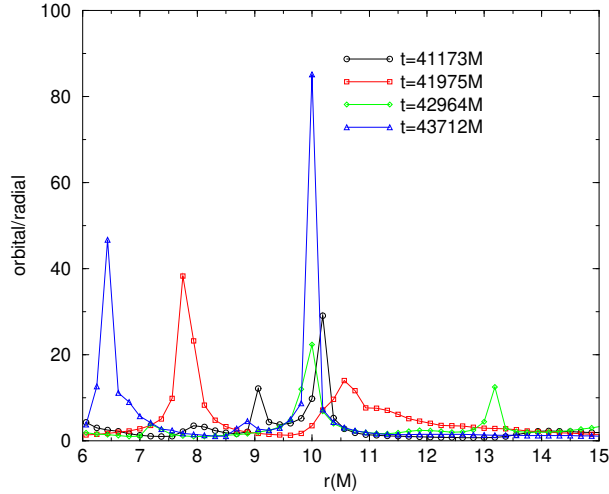


Fig. 9. Shows the time evolution of ratio of frequencies computed from numerically modeled accretion disk which included tori around the black hole at a fixed radial distance, The location of different ratios stay in one place with the small oscillation around the  $10.2M$  There are some other ratios which can also be seen but they are not stay at a fixed  $r$ . The variation of ration at  $10.2M$  in different times shows the vertical oscillation of torus around the non-rotating black hole. The lower of the frequencies may reflect changes in the emissivity of the torus.

in different ratios and high frequency signature can also be a specific signature of a microquasar (both GRO *J1655 – 40* and GRS 1915 + 105).

In two discovered transients, XTE *J1550 – 564* and XTE *J1859 + 226*, the QPO frequency substantially changes from observation to observation. The frequencies of XTE *J1550 – 564* have been measure 276 Hz for vertical and 184 Hz for radial<sup>21</sup>. Depend on the mass of observed black hole, vertical and radial frequencies can be changed in XTE *J1859 + 226* black hole binaries. Ref.26 report the measurement of a single high frequency QPO at 187 Hz associated with XTE *J1859 + 226*. If the 187 Hz frequency corresponds to the vertical epicyclic 3 : 2 resonance, the second high frequency QPO at 125 Hz, which is the radial epicyclic of oscillation. On the other side, if the 187 Hz frequency is the result of radial epicyclic frequency, the expected vertical epicyclic frequency is at 281 Hz. These sources also exhibit pairs of QPOs that have commensurate frequencies in a 3 : 2 ratio.

Commensurate high frequency QPO frequencies can be seen as a signature of an oscillation driven by some type of resonance conditions. Ref.27 had proposed that QPOs could represents a resonance in the coordinate frequencies given by general relativistic motions close the black hole.

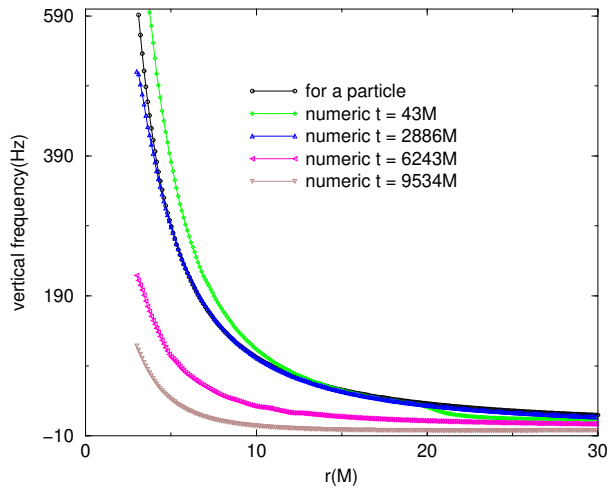


Fig. 10. Orbital frequencies plotted for analytic and numerical considerations at different times as a function of radial dependence. Comparison of the orbital epicyclic frequencies of a test particle with a perfect fluid disk case for star disk interaction processes produced from fully general relativistic hydrodynamic code. There is a one-armed spiral shock wave is created on the accretion disk, seen in Donmez, 2006 (in press). It causes to loose to mass of black hole and reduces to epicyclic frequency of accretion disk during the time evolution. For both cases, the mass of the black hole is  $M = 10M_{\odot}$  and  $a = 0.0$  which is the Schwarzschild black hole.

## 5. Conclusion

The oscillations of fluid confined by gravity and centrifugal forces can lead to rich behavior under a variety of astrophysical scenarios, QPOs in X ray binaries. It is plausible that the characteristic frequencies of the collective motion manifests itself in X-ray luminosity variation. Under quite general considerations we have shown that simple, acoustic modes which have their origin in free particle oscillations are modified by the hydrodynamics and can couple to one another in non linear fashion. The locking of excited modes could explain the fact that the observed QPO frequencies drift over considerable ranges while still arising from resonant interactions. We believe that their signature is present in the observations of accretion flows in strong gravitational fields, and will allow for the measurement of important parameters related to the black hole. The strong- field effects of general relativity and in particular metric properties of space-time around the black hole make the excitation of a 3:1 or 3:2 anharmonic epicyclic resonance, driven by orbital motion whose orbital frequency may be imprinted on the X-ray flux as a fairly prominent QPOs.

We have shown here that the tori and shock wave created on the accretion

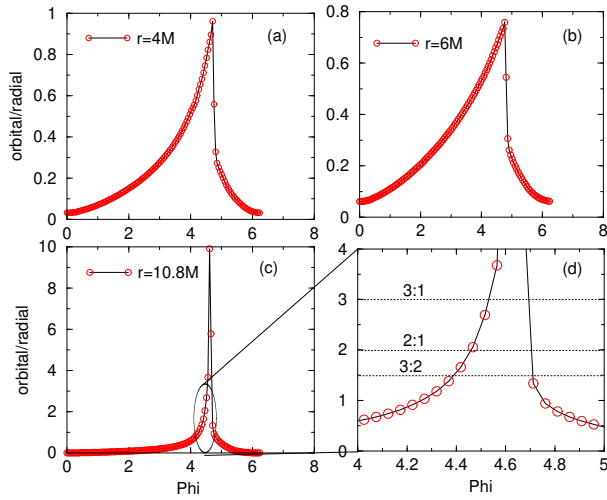


Fig. 11. The ratio of orbital to radial frequencies in the accretion disk which is produced by general relativistic hydrodynamics code as a results of star-disk interaction. The numerical results used here are taken from Donmez, 2006 (in press), seen in Fig.3 at  $t = 9534.70M1M$  which shows the created one armed-spiral shock wave around the non-rotating black hole. The ratio of frequency are plotted as a function of angular distance at a fixed  $r$ . (a)shows the ratio at  $r = 4M$ . It is inside the last stable circular orbit and the ratio is  $< 1$ . (b)shows the ratio at  $r = 6M$ . It is on the last stable circular orbit and the ratio is also  $< 1$ . (c)shows the ratio at  $r = 10.8M$ . It is outside the last stable circular orbit and the ratio has  $> 1$  values. It means that we have different orbits. (d) we have focused around  $\phi = 4.5$  where there is a pick. We have also pointed the orbits 2 : 1, 3 : 1 and 3 : 2.

16 *Donmez, O.*

disk around the black hole produces oscillatory behavior. These types of structures constitute radial pressure gradients. So the pressure gradients themselves can permit the existence of discrete modes. As a consequence of these dynamics, X-rays can

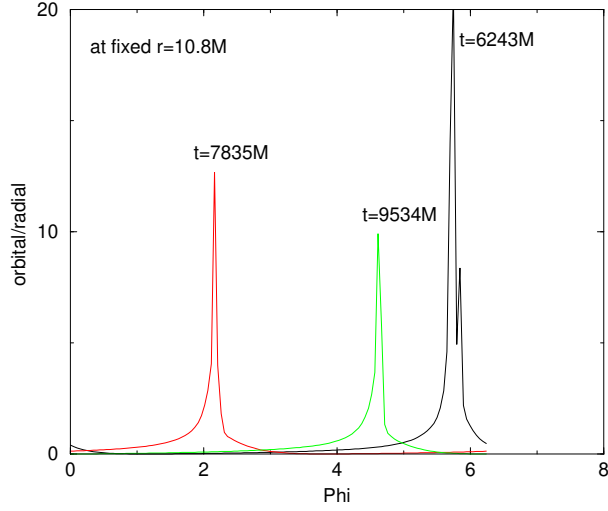


Fig. 12. Shows the time evolution of ratio of frequencies computed from star-disk interaction at a fixed radial distance,  $r = 10.8M$ . The location of 3:2 ratios stay in one place but it is moving in angular direction after one-armed shock wave created which moves around the black hole. The times  $6243M = 0.306$  second,  $7835M = 0.385$  second and  $9534M = 0.468$  second calculated for the black hole,  $M = 10M_{\odot}$ .

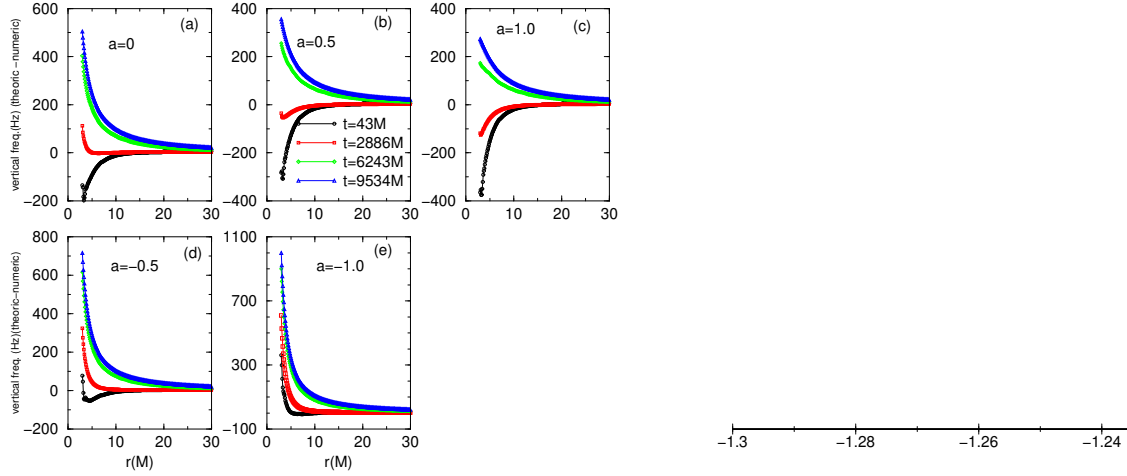


Fig. 13. Same data used in Fig.10 but difference between theoretical and numerical results are plotted as a function of  $r$  at different times.

be emitted by black hole binary system. The results of these different dynamical structures on the accretion disk responsible for QPOs are discussed in detail. The observed frequency ratios are consistent with the computed numerical values. On the other hand, our numerical results exhibits different commensurate frequencies in 4 : 1, 5 : 1..., seen in Figs.9 and 12.

## References

1. Dönmez, O., IJMPD (Submitted)
2. Dönmez, O., *Astrophysics and Space Science*, in press.
3. van der Klis M., *Ann. Rev of A&A* **38** (2000), 717.
4. McCalum, J., E., and Remillard, R., A., (2003) astro-ph/0306213.
5. Wagoner, R., V., *Physics reports* **311** (1999), 259.
6. Kato, S., *PASJ* **53** (2001), 1.
7. Dönmez, O., IJMD, in press.
8. Dönmez, O., IJMD (Submitted).
9. Dönmez, O., *Applied Mathematics and Computations* **175** (2006), 902-922.
10. Giannios, D., & Spruit, H. C., *A&A* **427** (2004), 251.
11. Lee, W. H., Abramowicz, M. A., & Kluzniak, W., *ApJ* **603** (2004), L93.
12. Kluzniak, W., Abramowicz, M. A., Kato, S., Lee, W. H., & Stergioulas, N., *ApJ* **603** (2004), L89.
13. Zanotti, O., Rezzolla, L., & Font, J. A., *MNRAS* **341** (2003), 832.
14. Bardeen, J., M., Press, W., H., & Teukolsky, S., A., *ApJ* **178** (1972), 347.
15. Okazaki, A., T., Kato, S., & Fuke, J., *PASJ* **39** (1987), 457
16. Amin, A., M., & Frolov, A., V., astro-ph/0603687
17. Kato, S., Mineshige, J., *Black Hole Accretion Disks*, Kyoto University press: Kyoto, 1998.
18. Rezzolla, L., Yoshida, S., and Zanotti, O., *MNRAS* **344** (2003), 978.
19. Dönmez, O., *Astrophysics and Space Science* **293** (2004), 323-354.
20. Abramowicz, M., A., and Kluzniak, W., *A&A* **374** (2001), L19-L20.
21. Remillard, R., A., Munro, M., P., McClintock, J., E., Orosz, J., A., *ApJ* **580** (2002), 1030-1042.
22. Aschenbach, B., *A&A* **425** (2004), 1075-1082.
23. Qian, L., and Wu, Xue-Bing, *Chinese Journal of Astronomy and Astrophysics* **5** (2005), 258-262
24. Strohmayer, T., E., *ApJ* **552** (2001a) L49.
25. McClintock, J., E., and Remillard, R., A., (2004), astro-ph/0306213.
26. Cui, W., Shrader, C., R., Haswell, C., A., Hynes, R., I., *ApJ* **535** (2002), L123.
27. Abramowicz, M., A., and Kluzniak W., *A&A* **374** (2001), L19.